PTFE-Based Core−Soft Shell Nanospheres and Soft Matrix Nanocomposites

Katia Sparnacci, Diego Antonioli, Simone Deregibus, and Michele Laus*

Dipartimento di Scienze dell' Ambiente e della Vita, Via G. Bellini 25 g, Università del Piemonte Orientale "A. Avogadro", INSTM, UdR Alessandria, 15100 Alessandria, Italy

Tiziana Poggio, Valeri Kapeliouchko, and Giovanna Palamone

Solvay Solexis SpA, Piazzale Donegani 5/6, 15047 Spinetta Marengo, Alessandria, Italy

Giampaolo Zuccheri and Rosita Passeri

Dipartimento di Biochimica "G. Moruzzi", S3 center of the National Institute for the Physics of the Matter (CNR), Italian Interuniversity Consortium for Materials Science and Technology (INSTM) at the University of Bologna. Via Irnerio 48, 40126 Bologna, Italy

Received December 29, 2008; Revised Manuscript Received March 30, 2009

ABSTRACT: A PTFE latex, with particles in the submicrometer size range, was employed as seed in the emulsifier-free emulsion copolymerization of two mixtures of acrylic and methacrylic comonomers to obtain PTFE-based core−soft shell nanoparticles. Stable latexes were obtained. By appropriately choosing the ratio between the comonomers and the PTFE seed in the reaction mixture, it was possible to obtain particles with various sizes and a narrow size distribution. The shell is swollen in water due to the presence of the ionic methacrylic acid units. A fractionated-type crystallization phenomenon of the PTFE component was observed and is ascribed to the small size of the PTFE material. The low glass transition temperatures of the shell forming materials could permit the preparation of soft matrix nanostructured films by latex deposition and water evaporation.

Introduction

Fluorinated polymers, and among them poly(tetrafluoroethylene) (PTFE), are particularly attractive and versatile compounds because of their unique properties linked to the low polarizability and the high bond energy of the C−F bond (486 kJ/mol) as well as the perfect shielding of the C−C backbone by the fluorine atoms.[1,2] The peculiar combination of low friction coefficient, surface energy and dielectric constant, low refractive index, low flammability, low moisture adsorption and excellent thermal stability and inertness to solvents, hydrocarbons, acids and alkalies resulted in major applications in modern technologies ranging from building, automotive and aerospace industries to optics and microelectronics. In addition, new application opportunities are emerging for these materials including ultralow-K dielectric materials, nanofillers for fluoroelastomers and fire retardant additives that can inhibit the dripping of molten particulates from the burning polymers.[3−5] However, for these applications the compatibility and the adhesion properties are inadequate. In particular, the low adhesion and wettability of the PTFE result in a low degree of dispersion within the matrix and the poor compatibility leads to an inefficient mechanical coupling among the various blend components. Moreover, the resulting compositions exhibit a pearlescent opaque appearance that prevents their use in applications where transparency is required. Finally, the poor dispersion of PTFE material adversely affects the efficiency in reducing the heat release.

To enhance wettability and compatibility, several PTFE surface modification strategies were developed requiring high reactive chemicals[6,7] or high energy inputs (plasma or UV).[8−10] In particular, plasma-assisted techniques were used to modify a thin surface layer while preserving the bulk properties. For example, core−shell nanoparticles consisting of a PTFE core and a thin PMMA shell, were prepared through grafting reactions of hydrocarbon monomers on preirradiated PTFE, in CO_2/aqueous system.[10] Interesting and promising results were recently described in the preparation of compounds of electron-beam-irradiated PTFE and polyamide (PA) obtained by reactive extrusion.[11,12] The occurrence of transamidation reactions accompanied by the breakdown of the PTFE agglomerates resulted in a very good dispersion degree of PTFE within the PA matrix thus ultimately leading to compounds with improved mechanical properties. However, it appears quite difficult to obtain stable and homogeneous surface modifications. A consistent degradation of the basic PTFE structure upon irradiation is unavoidable, thus leading to substantial changes in several PTFE characteristics including its melting and crystallization behaviors.

A promising nondestructive alternative to produce compounds featuring a perfect distribution of PTFE particles is based on the preparation of core−shell particles in which the core is constituted by PTFE and the shell by a conventional polymer. A perfect degree of dispersion of the core−shell particles within a polymer matrix could be obtained if the shell is constituted by the same polymeric material with which the polymer matrix is made up. The application of this concept would lead to a novel class of specific and very efficient PTFE-based additives.

An additional reason of interest for these systems is also related to their potential use as building blocks for colloidal crystals and other nanostructured materials.[13−15] In fact, provided that dimensional and compositional homogeneity is obtained, the core−shell particles should be able to self-assemble to generate a highly ordered structure. If the flow transition temperature of the shell-forming polymer is lower than the one of the core, annealing at a temperature intermediate between the two, allows the shell-forming polymer to soften and form a matrix surrounding a 3D periodic array in which the cores are

* Corresponding author. Telephone: +390131360255. Fax: +390131360250. E-mail: laus@mfn.unipmn.it.

10.1021/ma802871y CCC: $40.75
Published on Web 04/20/2009

Table 1. Synthesis Details, Yield, and Solid Content of the Various Samples

comonomer mixture	sample	volume of water (mL)	volume of comonomer mixture (mL)	volume of PTFE latex (mL)	yield (%)	solid content (g/mL)
C1	PC1	500	70.0	0	90.2	0.110
	3MDC1	494	70.0	5.8	82.3	0.101
	6MDC1	488	70.0	12.0	98.9	0.104
	12MDC1	474	70.0	25.6	83.3	0.106
	18MDC1	459	70.0	41.2	81.5	0.085
	30MDC1	420	70.0	80.5	91.6	0.093
	40MDC1	375	70.0	125.3	92.7	0.0104
	50MDC1	312	70.0	188.0	85.0	0.098
	60MDC1	218	70.0	282.0	80.4	0.095
	70MDC1	61	70.0	439.0	84.6	0.106
C2	PC2	500	70.0	0	81.5	0.113
	3MDC2	494	70.0	5.8	90.8	0.108
	6MDC2	488	70.0	11.5	92.3	0.116
	12MDC2	476	70.0	24.5	88.4	0.111
	18MDC2	468	70.0	39.5	79.5	0.099
	30MDC2	445	70.0	55.4	81.6	0.115
	40MDC2	380	70.0	120.7	95.6	0.102
	50MDC2	319	70.0	181.0	97.1	0.1130
	60MDC2	229	70.0	271.4	88.3	0.109
	70MDC2	78	70.0	422.3	81.5	0.126

arranged in regular registry. Since the characteristic size of the different domains is on the nanometer range, photonic properties are originated from the periodic modulation in structure and composition.

The most common and versatile approach to obtain such core−shell architectures is the seed emulsion polymerization. In early studies, several composite particles consisting of PTFE core and cross-linked polybutadiene shell were described by Okaniwa[16] whereas the preparation of one sample only of core−shell particles with the core made up of PTFE and the shell of cross-linked polystyrene, was reported by Othegraven.[17] More recently, extensive studies were reported for core−shell nanoparticle systems composed of PTFE core and polystyrene[18] or polyacrylic shell[19−21] with various compositions.

Solvay Solexis developed[22,23] the tetrafluoroethylene (TFE) homo- and copolymerization microemulsion technology, on industrial scale, based on the use of perfluoropolyethers (PFPE) in oil/water microemulsion. Polytetrafluoroethylene (PTFE) aqueous dispersions were obtained, with the particle concentration number as high as $10^{18}-10^{19}$ per liter, and the particle size as small as 10 nm. Moreover, by varying the amount and type of PFPE as well as the quantity and nature of the comonomers, PTFE particles with a great morphological diversity were obtained.

Within an investigation aimed at the assessment of the macromolecular engineering potential in the design of PTFE-based core−shell nanoparticles and related nanomaterials, PTFE latexes with particles in the submicrometer size range, were employed as seeds in the emulsifier-free emulsion polymerization of several vinyl monomers. This could lead to a great variety of complex macromolecular structures with novel and unusual properties.[24−26]

In this general frame, the present paper describes the preparation and some physicochemical characteristics of two systems obtained by emulsifier-free emulsion copolymerization using a PTFE latex, with nearly monodisperse spherical particles of 41 nm diameter, as the seed for the copolymerization of acrylic and methacrylic monomers. The acrylic and methacrylic comonomer systems were selected to lead to low glass transition temperature materials. Accordingly, the preparation of core−soft shell nanospheres and soft matrix nanocomposites can be anticipated. These particles, combining the properties of an easily film forming latex with a stabilizing high T_g component, present, among others, potential industrial interest in paint and coating technology.

Experimental Section

Materials. The monomers butylacrylate (≥99%, Aldrich), methylacrylate (≥99%, Fluka), ethylacrylate (≥99%, Fluka) were distilled under reduced pressure in nitrogen atmosphere and stored at −18 °C until use. Methacrylic acid (≥98.0%, Fluka) and potassium persulfate (98%, Carlo Erba) were used without further purification. The PTFE latex employed in this study, marked MD, was provided from Solvay Solexis, and prepared by nanoemulsion polymerization of tetrafluoroethylene (TFE) as previously reported.[18]

The latex MD is a stable colloidal dispersion of PTFE in water, with no free surfactant detectable. It has a mean particles diameter of 41 nm (as determined by photon correlation spectroscopy, PCS), and a solid content of 347.6 g/L corresponding to a number of particles per liter of 3.1×10^{18}. The conductivity of the latex is 860 μS/cm.

Preparation of Core−Soft Shell Nanospheres. The core−shell latexes were synthesized by emulsifier-free batch seeded emulsion polymerization with PTFE seed particles. All the polymerizations were carried out at 75 °C in a 1 L five-neck jacketed reactor equipped with a condenser, a mechanical stirrer, a thermometer and inlets for nitrogen and monomers. The appropriate amount of PTFE latex was introduced into the reactor and deionized water was added until a total volume of 500 mL was reached. The mixture was purged with nitrogen and nitrogen was fluxed during the entire polymerization reaction. The reaction mixture was then heated to 75 °C, under the constant stirring rate of 300 rpm, and 70.0 mL of the comonomeric mixture was added dropwise at an addition rate comprised between 2.0 and 2.5 mL/min. In particular, two comonomer mixtures were employed, marked C1 and C2. The C1 mixture is constituted by methylacrylate, ethylacrylate and methacrylic acid with weight percent of 39%, 57% and 4%. The C2 mixture is constituted by butylacrylate and methacrilic acid with weight percent of 96% and 4%. After an additional 15 min of equilibration time, a potassium persulfate aqueous solution (10.0 mL, 0.74 mmol) was added, and the reaction was allowed to proceed for 24 h. At the end of the reaction, the latexes were purified by repeated dialyses. All the latexes were obtained following the above general procedure. The amount of the potassium persulfate aqueous solution and the comonomeric mixture volume was kept constant (70.0 mL corresponding to 65.4 g for C1 and 62.6 g for C2 mixture) and the initial PTFE latex amount was varied. Table 1 reports the detailed experimental conditions for the various preparations, including yield and solid content.

Preparation of PC1 and PC2 Latexes. Two reference samples, marked PC1 and PC2, were prepared starting from the two comonomer mixtures C1 and C2. These latexes were synthesized in the same experimental conditions employed for the preparation

of sample series *n*MDC1 and *n*MDC2 but without the PTFE seed. Both polymerizations were carried out at 75 °C in a 1 L five-neck jacketed reactor equipped with a condenser, a mechanical stirrer, a thermometer and inlets for nitrogen and monomers. 500 mL of deionized water were introduced into the reactor, heated to 75 °C and purged with nitrogen. Then, 70.0 mL of either one of C1 and C2 monomer mixtures were added dropwise under the constant stirring of 300 rpm at an addition rate comprised between 2.0 and 2.5 mL/min. After additional 15 min equilibration time, a potassium persulfate aqueous solution (10 mL, 0.74 mmol) was added and the mixture was let to react for 24 h. Then, the latexes were purified from the unreacted monomers by repeated dialyses.

Characterization. MD particle size and size distribution were measured by transmission electron microscope (TEM). TEM images were obtained using a Philips CM10. The particle size and size distribution of the core−soft shell particles were determined by photon correlation spectroscopy (PCS) analysis at 25 °C, with a Malvern Zetasizer 3000 HS at a fixed scattering angle of 90°, using a 10 mW He−Ne laser and PCS software for Windows (version 1.34, Malvern, U.K.). Each value is the average of five measurements. The instrument was checked with a standard polystyrene latex with a diameter of 200 nm. Electrophoretic mobility was measured with a Malvern Zetasizer 3000 HS. Each value is the average of five measurements. Average molar masses were determined by SEC of THF solutions with a 590 Waters chromatograph equipped with refractive index and ultraviolet detectors, using PLgel 10^3, 10^4, 10^5, and 10^6 Å columns calibrated with PS standard samples. For the determination of the copolymer molar masses, 10.0 mL of THF was added to about 100 mg of the core−shell sample. After centrifugation at 18000 RCF for 20 min, quantitative sedimentation of the PTFE was obtained. Then, the supernatant was withdrawn and the solvent evaporated under reduced pressure.

Thermogravimetric analysis (TGA) was performed with a Mettler-Toledo TGA/SDTA851^e at a scanning rate of 10 °C/min from room temperature up to 1100 °C under nitrogen flow. The solid content of latex dispersions was determined by TGA. Differential scanning calorimetry (DSC) was carried out using a Mettler-Toledo DSC 821 apparatus. Samples of about 5 mg were employed. The instrument was calibrated with high purity standards at 10 °C/min. Dry nitrogen was used as purge gas.

AFM analysis was performed on a Multimode Nanoscope IIIa instrument (Veeco, Santa Barbara, CA). A multilayer of nanoparticles is obtained by drop-casting an aliquot of water suspension on a disk of freshly cleaved muscovite mica (Electron Microscopy Sciences, Hatfield, PA) and letting the solvent evaporate slowly. The spread is then imaged in tapping-mode atomic force microscopy in air operating in constant amplitude mode. Images are then subjected to flattening using the microscope constructor software. Particle locations are semiautomatically measured using a custom-developed software tool.[27]

Results and Discussion

The PTFE MD latex consists of spherical particles with average diameter of 41 nm and narrow size distribution, as illustrated by the TEM micrograph of Figure 1, and does not contain free residual surfactant.

The core−shell nanospheres were obtained via emulsifier-free seeded emulsion polymerizations. The appropriate amounts of the acrylate and methacrylate comonomeric mixtures were added dropwise to a water suspension containing the appropriate amount of PTFE latex. Potassium persulfate was the free radical source. Two comonomer mixtures were employed, identified as C1 and C2. The C1 mixture is constituted by methylacrylate, ethylacrylate and methacrilic acid with weight percent of 39%, 57%, and 4%. The C2 mixture is constituted by butylacrylate and methacrilic acid with weight percent of 96% and 4%. Starting from the two comonomer mixtures, C1 and C2, two latex sample series were obtained marked *n*MDC1 and *n*MDC2, where *n* represents the PTFE weight percent with respect to the total weight of the comonomers and PTFE initially added,

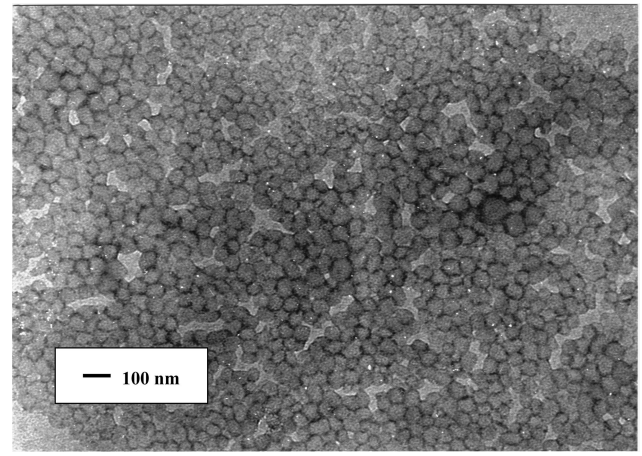

Figure 1. TEM micrograph of sample MD.

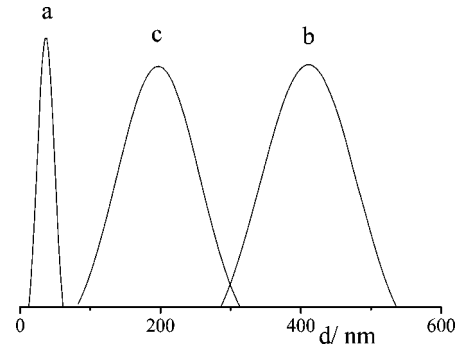

Figure 2. PCS spectra of latex MD (a) and samples 6MDC1 (b) and 18MDC1 (c).

MD indicates the PTFE latex employed in this study, and C1 and C2 identify the specific comonomer mixture. No trace of gel or polymeric gross aggregates was found in all cases. Nearly quantitative monomer conversion and nanosphere yield were obtained. The final latexes are very stable (up to 2 years).

The particle size and size distribution of all the core−shell samples were determined by photon correlation spectroscopy (PCS), and are reported in Table 2. Diameters ranging from 61 to 372 nm are obtained with polydispersity index ranging from 0.012 to 0.260. As a typical example, Figure 2 reports the PCS curve of samples 6MDC1 and 18MDC1 and, for comparison, of MD latex. No residual PTFE deriving from MD latex is present in the various samples thus indicating that PTFE is highly efficient as seed. The monomodal and narrow size distribution of the latex particles suggests that the emulsion copolymerization occurs quantitatively onto the PTFE seeds, possibly because of the great seed surface area available due to the small size of the particles. This is in qualitative agreement with theoretical[28,29] and experimental results.[21]

In this respect, it should be observed that the complete immiscibility of PTFE particles in the monomer mixtures avoids diffusion of the growing macroradicals inside the seed thus further helping the formation of a purely core−shell morphology.

The nanosphere composition was determined by thermogravimetric (TGA) analysis. As a typical example, Figure 3 reports the TGA curves of *n*MDC2 sample series. For comparison, the TGA curves of latex MD and the TGA curve of the blank sample PC2 are included.

As the weight losses at 400 and 580 °C are assignable to PC2 copolymer and PTFE decomposition, respectively, it is clear that the PTFE weight loss increases proportionally to the fraction of PTFE. The presence of the PTFE does not substantially

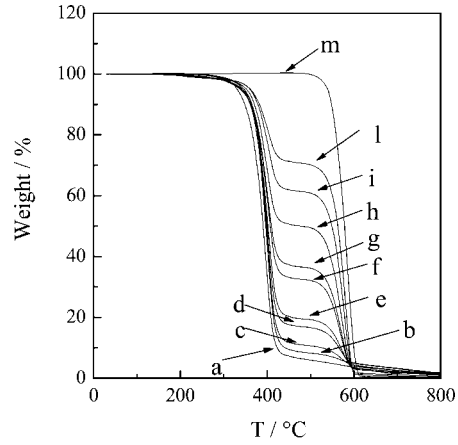

Figure 3. TGA curves at 10 °C/min heating rate for various samples: PC2 (a); 3MDC2 (b); 6MDC2 (c); 12MDC2 (d); 18MDC2 (e); 30MDC2 (f); 40MDC2 (g); 50MDC2 (h); 60MDC2 (i); 70MDC2 (l); MD10 (m).

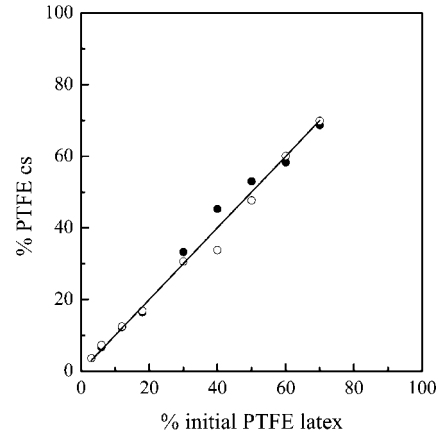

Figure 4. PTFE in the core−shell samples for *n*MDC1 (●) and *n*MDC2 (○) series estimated by TGA and calculated (−) from the synthetic conditions as a function of the amount of initially added PTFE latex.

modify the thermal stability of the PC2 copolymer layer thus indicating a low, if any, interaction between the PTFE core and the shell-forming polymeric material.

Figure 4 reports collectively the composition data of both *n*MDC1 and *n*MDC2 sample series estimated by TGA and calculated on the base of the amount of the feed components as a function of the amount of the initially added PTFE. For both sample series, the predicted and estimated data are in good agreement.

This result is obvious in case of nearly quantitative yield, but it represents an additional confirmation that no loss of PTFE occurred even in samples containing the lowest PTFE amount, an indirect indication that the core and the shell materials are bound.

Figure 5 illustrates the trend of the particle diameter for both sample series as a function of the weight percent of the fed PTFE. In both series, the particle diameter decreases, steeply at first and then more gradually, as expected, the initial PTFE amount increases.

However, for both sample series, the particle size estimated assuming the presence of core−shell nanospheres only and quantitative yield, is definitely lower than the values experimentally determined by PCS. For example, a core−shell sample obtained from a 6% MD latex content and methyl methacrylate as the shell forming monomer presents a particle diameter of

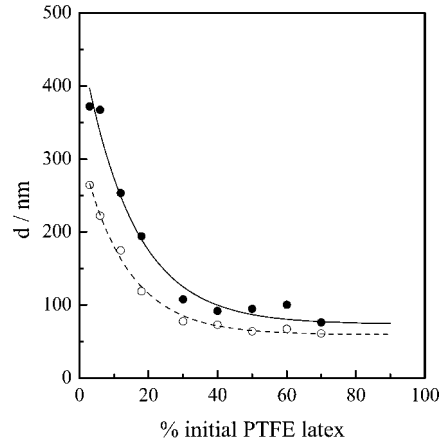

Figure 5. Trend of the particle diameter in the various sample series as a function of the amount of initially added PTFE latex as determined by PCS: *n*MDC1 (●); *n*MDC2, (○).

141 nm (manuscript in preparation), whereas samples 6MDC1 and 6MDC2 present diameters of 367 and 222 nm, respectively. Furthermore, the size of samples belonging to *n*MDC1series is always higher than the one of the corresponding samples of *n*MDC2 series. These two observations suggest that in both sample series, the shell is swollen in water possibly due to the

Table 2. Size, Polydispersity Index, ζ-Potential, Glass Transition Temperature, Weight Average Molecular Weights, Polydispersity Index, and Sample Composition Derived from TGA of the Various Samples

sample	*d*(PCS) (nm)	polydispersity index (PCS)	ζ-potential (mV)	T_g (°C)	M_w	PI	TGA comp (%)
PC1	933	0.110	−73.4	7	1.53E+06	5.2	
3MDC1	372	0.111	−71.5	−3	1.35E+06	5.1	1.6
6MDC1	367	0.035	−66.9	11	7.42E+05	4.5	6.7
12MDC1	253	0.016	−65.8	13	1.30E+06	5.1	12.3
18MDC1	194	0.063	−67.3	8	1.00E+06	5.5	16.5
30MDC1	108	0.124	−71.6	12	1.38E+06	6.0	33.3
40MDC1	92	0.103	−69.4	13	9.81E+05	6.4	45.3
50MDC1	95	0.106	−65.7	12	1.38E+06	5.0	53.0
60MDC1	100	0.103	−67.8	15	8.13E+05	4.4	58.3
70MDC1	76	0.104	−69.3	13	6.22E+05	4.0	68.7
PC2	714	0.055	−76.3	−37	1.74E+06	5.4	-
3MDC2	264	0.017	−78.3	−33	1.39E+06	6.5	3.6
6MDC2	222	0.014	−72.4	−37	1.07E+06	7.2	7.3
12MDC2	175	0.118	−65.0	−38	1.25E+06	4.9	12.5
18MDC2	119	0.012	−66.7	−39	1.12E+06	6.9	16.9
30MDC2	78	0.037	−72.5	−39	9.86E+05	4.0	30.6
40MDC2	73	0.035	−68.3	−35	7.63E+05	3.6	33.8
50MDC2	64	0.106	−66.9	−38	1.17E+06	6.3	47.7
60MDC2	67	0.109	−66.3	−40	1.33E+06	7.5	60.1
70MDC2	61	0.096	−67.6	−40	6.10E+05	4.0	69.9

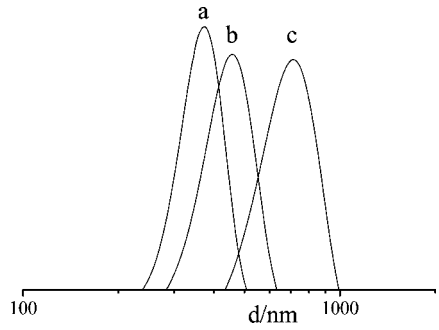

Figure 6. PCS curves of sample 3MDC1 at pH 5.0 (a) and at pH 9.0 after 12 (b) and 48 h (c) equilibration time.

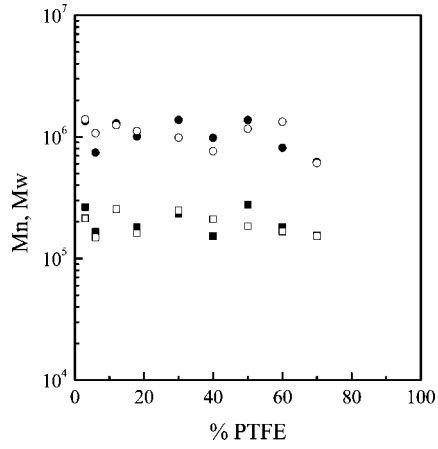

Figure 7. Trends of M_n (square) and M_w (circle) in the various sample series as a function of the amount of initially added PTFE latex: *n*MDC1 (full symbols); *n*MDC2 (open symbols).

presence of the ionic and pH sensitive methacrylic acid units. The swelling degree appears lower for series *n*MDC2 due to the presence of butylacrylate units which are less hydrophilic than methyl- or ethylacrylate units which constitute the shell of the *n*MDC1 series.

PCS measurements performed at different pH values confirmed the occurrence of some degree of swelling. Figure 6a reports the PCS curve of the sample 3MDC1 at the initial pH of 5.0. Then, the pH was adjusted to 9.0 by addition of NaOH and the PCS measurement was repeated after 12 and 48 h equilibration time leading to curves 6b and 6c, respectively.

The PCS curves appear regularly shifted toward higher values along the size scale, and correspondingly broadened, as the equilibration time increases thus clearly indicating that the sample undergoes a slow swelling process. Then, the pH was again set to 5.0 and after 24 h the PCS measure was repeated, leading to an average size of 380 nm. This value is very similar to the initial one, thus indicating that the swelling process is reversible.

For the core−shell sample series *n*MDC1 and *n*MDC2, the shell forming material was separated from PTFE through addition of THF and centrifugation at 18000 RCF. In these conditions, quantitative sedimentation of PTFE was obtained and the shell forming material was recovered from the supernatant, thus making it possible to obtain information about the molar mass and molar mass distribution of the shell material via SEC. The molar mass characteristics of the shell forming material in the *n*MDC1 and *n*MDC2 core−shell nanoparticles are illustrated in Figure 7. M_n and M_w do not depend on the amount of added PTFE and are quite similar in both series.

The thermal behavior of the various samples was investigated by differential scanning calorimetry (DSC). The MD and the core−shell samples were subjected to a thermal cycle consisting of a first heating at 20 °C/min to 340 °C, to cancel the thermal history, first cooling at −10 °C/min to −65 °C and second heating at 10 °C/min to 340 °C. Samples PC1 and PC2 were subjected to a thermal cycle consisting of a first heating at 20 °C/min to 140 °C, first cooling at −10 °C/min to −65 °C and second heating at 10 °C/min to 140 °C. Figure 8 reports the DSC second heating (at 10 °C/min) of samples MD and 12MDC1. The same Figure reports the second heating curve of sample PC1.

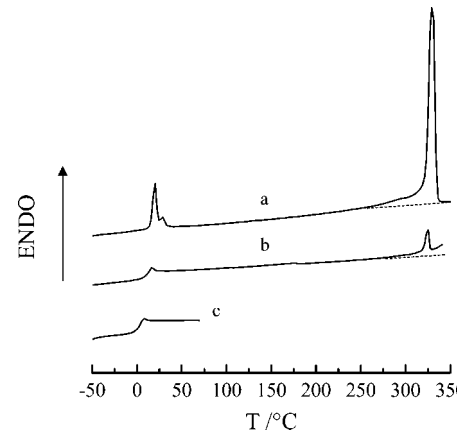

Figure 8. DSC second heating at 10 °C/min of samples MD (a), 12MDC1 (b), and PC1 (c).

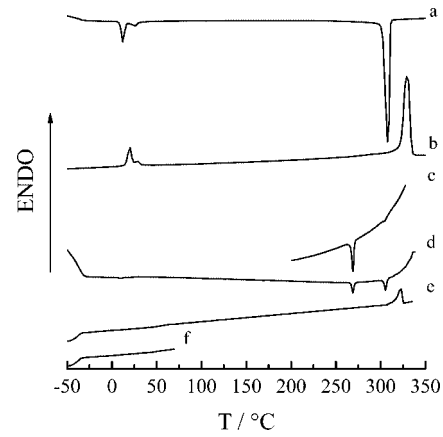

Figure 9. DSC first cooling (a) and second heating (b) of sample MD, first cooling after fast heating (c), first cooling (d), and second heating (e) of sample 6MDC2 and second heating (f) of sample PC2. All the DSC runs were performed at 10 °C/min.

At low temperature, sample 12MDC1 presents a complex thermal phenomenology consisting in the glass transition of the C1 shell-forming material at about 10 °C partly superposed to an endothermic transition structured in two overlapping components attributed to the PTFE core by direct comparison with the DSC thermogram of the MD sample. The melting of the PTFE core in sample 12MDC1 occurs at 324 °C, i.e., at the same temperature of the MD sample. However, a drift in the DSC baseline is observed in all the core−shell samples at temperatures above 300 °C. This drift is attributed to the thermal decomposition of the shell forming materials as also confirmed by the relevant TGA data. The glass transition of C2 shell-forming material occurs at −36 °C (Figure 9f) that is well apart from the low temperature transition of the PTFE. Consequently, in samples *n*MDC2 the thermal transitions pertaining to the core- and shell-forming materials are well resolved as illustrated in Figure 9d for sample 6MDC2, as a typical example.

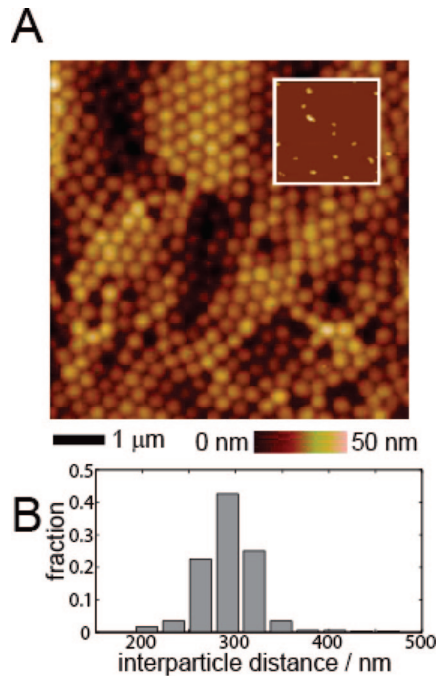

Figure 10. AFM image and interparticle distance distribution for the 3MDC1 specimen. (A) Tapping-mode AFM image obtained from a film of core−shell nanoparticles that has been obtained from room-temperature slow solvent evaporation on a drop-casted spread on a freshly cleaved muscovite mica disk. Heights are coded in shades according to the reported colorbar. In the inset, a TM-AFM image of the MD seeds on mica, reported on the same size scale for comparison. (B) distribution of the minimum interparticle distances (center-to-center) for the nanoparticle in part A.

For sample MD alone, the crystallization process occurs at 305 °C (Figure 9a), in agreement with literature data,[18,30] whereas, in the case of sample 6MDC2 a very peculiar crystallization phenomenology is also observed (Figure 9, parts c and d).

In particular, when the DSC cooling curve is recorded after fast heating (150 °C/min) the sample to a temperature just above the melting of the PTFE, a single crystallization exotherm at 270 °C is observed. In contrast, when the DSC heating rate is 10 °C/min, two crystallization peaks at 270 and 305 °C are observed. This complex crystallization behavior was also described in PTFE/PS core−shell nanospheres as well as in PTFE dispersions prepared by reactive extrusion and was ascribed to the small size of the PTFE material. This material is in the form of individual core particles embedded within a shell or matrix, and this can lead to a fractionated-type crystallization mechanism.[31] In the present case, when the heating rate is sufficiently fast, the PTFE cores crystallize as individual particles leading to the crystallization peak at 270 °C whereas, when the sample remains at high temperature for a relatively long time period, due to the lower DSC heating rate, the polyacrylic shell undergoes a thermal decomposition and the cores partly coalesce thus leading to bigger PTFE domains which crystallize at the bulk crystallization temperature of 310 °C. The observation of a single crystallization exotherm at 270 °C in case of samples 3MDC1 and 3MDC2 is a clear proof of the perfect dispersion degree of PTFE obtained in these systems. Unfortunately, in the present system, the thermal decomposition of the shell-forming material hinders a more detailed study of this interesting behavior. However, it could be anticipated that in the case of PTFE/PMMA core−shell nanoparticles, the thermal stability of the shell is high enough to allow the PTFE crystallization behavior to be thoroughly investigated as will be described in a forthcoming paper.

Finally, a morphological analysis was performed on films using atomic force microscopy.[32] A tapping-mode AFM image obtained from a multilayer deposition of 3MDC1 is presented in Figure 10, together with an AFM micrograph of the MD seeds only (in the inset, on the same size scale).

The AFM topography has been recoded on the dried specimen and it evidences the close-packed ordering of nanoparticles (hexagonal close packing with some imperfections). The distribution of minimum interparticle distances of the packed nanoparticles (as an estimate of particle diameter, reported in Figure 10b) is in good agreement with the correspondent particle diameter reported in Figure 5 thus demonstrating that the control of shell thickness and the self-assembly of particles in layers is a viable route toward the regular and controlled spacing of the nanoparticle cores (invisible in the AFM images as embedded in the thick shell layers).

Conclusion

Emulsifier-free seeded emulsion polymerizations, leading to the core−soft shell nanospheres were performed by adding appropriate amounts of the PTFE latex and either one of two acrylate and methacrylate comonomeric mixtures constituted by methylacrylate, ethylacrylate and methacrilic acid or by butylacrylate and methacrilic acid. No gel trace or polymeric gross aggregates was found in all cases and the final conversion, which coincides with the nanosphere yield, was nearly quantitative. The emulsion copolymerization occurred quantitatively onto the PTFE seeds thus leading to the formation of a core−shell morphology. The shell is swollen in water due to the presence of the ionic methacrylic acid units. The swelling degree is pH sensitive. The swelling propensity was lower for series containing butyl acrylate units which are less hydrophilic that the methyl- or ethylacrylate units. The glass transition of the soft shell material was about 10 °C for the *n*MDC1 series and −36 °C for the *n*MDC2 series. Although the thermal stability of the shell-forming material is not high enough to fully elucidate the thermal behavior of the core−shell samples, a fractionated-type crystallization phenomenon of the PTFE component is observed which is associated to the small size of the PTFE material and to the thermal decomposition of the shell forming material during the DSC analysis.

The high structural regularity of the core−shell samples allows the preparation of film with a periodic distribution of the cores thus ultimately leading to a well structured 2D colloidal crystal.

Supporting Information Available: Text discussing the kinetic study and figures showing the polymerization kinetics of 3MDC1 and DSC curves relevant to the glass transition for both sample series. This material is available free of charge via the Internet at http://pubs.acs.org.

References and Notes

(1) Feiring, A. E.; Imbalzano, J. F.; Kerbow, D. L. *Adv. Fluoroplast. Plast. Eng.* **1994**, 27–29.
(2) Scheirs, J. *Modern Fluoropolymers*; Wiley: New York, 1997.
(3) Gozzi, G. US Patent 4,632,963, 1987.
(4) Albano, M.; Apostolo, M.; Arcella, V.; Marchese, E. US Patent 6,395,834, 2002.
(5) Roma, P.; Camino, G.; Luda, M. P. *Fire Mater.* **1997**, *21*, 199–204.
(6) Zhao, B.; Brittain, W. J.; Vogler, E. A. *Macromolecules* **1999**, *32*, 796–800.
(7) Ji, L. Y.; Kang, E. T.; Neoh, K. G.; Tan, K. L. *Langmuir* **2002**, *18*, 9035–9040.
(8) Akinay, E.; Tincer, T. *J. Appl. Polym. Sci.* **2001**, *79*, 816–826.
(9) Konig, U.; Nitschke, M.; Menning, A.; Eberth, G.; Pilz, M.; Arnhold, C.; Simon, F.; Adam, G.; Werner, C. *Colloids Surf., B* **2002**, *24*, 63.
(10) Kipp, B. E.; DeSimone, J. M.; Pochan, D. J.; Gido, S. P. *Abstr. Prep. Am Chem. Soc.* **1997**, *213*, 31.

(11) Pompe, G.; Häussler, L.; Pötschke, P.; Voigt, D.; Janke, A.; Geissler, U.; Hupfer, B.; Reinhardt, G.; Lehmann, D. *J. Appl. Polym. Sci.* **2005**, *98*, 1308–1316.
(12) Pompe, G.; Häussler, L.; Adam, G.; Eichhorn, K.-J.; Janke, A.; Hupfer, B.; Lehmann, D. *J. Appl. Polym. Sci.* **2005**, *98*, 1317–1324.
(13) Xia, Y.; Gates, B.; Yin, Y.; Lu, Y. *Adv. Mater.* **2000**, *12*, 693–713.
(14) Kalinina, O.; Kumacheva, E. *Chem. Mater.* **2001**, *13*, 35–38.
(15) Paquet, C.; Kumacheva, E. *Mater. Today* **2008**, *11*, 48–56.
(16) Okaniwa, M. *J. Appl. Polym. Sci.* **1998**, *68*, 185–190.
(17) Othegraven, J.; Piazza, R.; Bartsch, E. *Macromol. Symp.* **2000**, *151*, 515–525.
(18) Giani, E.; Sparnacci, K.; Laus, M.; Palamone, G.; Kapeliouchko, V.; Arcella, V. *Macromolecules* **2003**, *36*, 4360–4367.
(19) Cui, X.; Zhong, S.; Xu, J.; Wang, H. *Colloid Polym. Sci.* **2007**, *285*, 935–940.
(20) Cui, X.; Zhong, S.; Zhang, H.; Gu, Q.; Li, J.; Wang, H. *Polym. Adv. Tech.* **2007**, *18*, 544–548.
(21) Suresh, K. I.; Pakula, T.; Bartsch, E. *Macromol. React. Eng.* **2007**, *1*, 253–263.
(22) Giannetti, E.; Visca, M. US Patent 4,864,006, **1987**.
(23) Kapeliouchko, V.; Marchese, E.; Colaianna, P. EU Patent 969027.
(24) Palamone, G.; Kapeliouchko, V.; Laus M. US Patent 20050197426, **2005**.
(25) Palamone, G.; Poggio, T.; Kapeliouchko, V.; Laus M. EU Patent 1849809, **2006**.
(26) Schwab, T.; Weinberg, S.; Poggio, T.; Kapeliouchko V.; Laus, M. WO Patent 2007065880, **2007**.
(27) Vinelli, A.; Primiceri, E.; Brucale, M.; Zuccheri, G.; Samorì, B. *Microsc. Res. Technique* **2008**, *71*, 870–879.
(28) Rios, L.; Hidalgo, M.; Cavaille, J. Y.; Guillot, J.; Guyot, A.; Pichot, C. *Colloid Polym. Sci.* **1991**, *269*, 812–824.
(29) Gilbert, R. J. *Emulsion Polymerization: A Mechanistic Approach*; Academic Press: London, 1995.
(30) Wang, X. Q.; Chen, D. R.; Han, J. C.; Du, Y. D. *J. Appl. Polym. Sci.* **2002**, *83*, 990–996.
(31) Jin, Y.; Hiltner, A.; Baer, E. *J. Polym. Sci., Polym Phys.* **2007**, *45*, 1138–1151.
(32) Binnig, G.; Quate, C. F.; Gerber, C. *Phys. Rev. Lett.* **1986**, *56*, 930–936.

MA802871Y